Human Molecular Genetics, 2006, Vol. 15, No. 4 ***637–651***
doi:10.1093/hmg/ddi479
Advance Access published on January 10, 2006

Loss of emerin at the nuclear envelope disrupts the Rb1/E2F and MyoD pathways during muscle regeneration

Gisela Melcon[1,†], Serguei Kozlov[2,†], Dedra A. Cutler[2,3,†], Terry Sullivan[2], Lidia Hernandez[2], Po Zhao[1], Stephanie Mitchell[1,3], Gustavo Nader[1], Marina Bakay[1], Jeff N. Rottman[4], Eric P. Hoffman[1,3] and Colin L. Stewart[2,*]

[1]Research Center for Genetic Medicine, Children's National Medical Center, Washington DC, USA, [2]Laboratory of Cell and Developmental Biology, National Cancer Institute, Frederick, MD, USA, [3]Department of Genetics, The George Washington University, Washington DC, USA and [4]Department of Medicine, Vanderbilt University Medical Center, 2220 Pierce Avenue, Nashville, TN 37232-6300, USA

Received October 6, 2005; Revised and Accepted January 5, 2006

Emery–Dreifuss muscular dystrophy (EDMD1) is caused by mutations in either the X-linked gene emerin (*EMD*) or the autosomal lamin A/C (*LMNA*) gene. Here, we describe the derivation of mice lacking emerin in an attempt to derive a mouse model for EDMD1. Although mice lacking emerin show no overt pathology, muscle regeneration in these mice revealed defects. A bioinformatic array analysis of regenerating *Emd* null muscle revealed abnormalities in cell-cycle parameters and delayed myogenic differentiation, which were associated with perturbations to transcriptional pathways regulated by the retinoblastoma (Rb1) and MyoD genes. Temporal activation of MyoD transcriptional targets was significantly delayed, whereas targets of the Rb1/E2F transcriptional repressor complex remained inappropriately active. The inappropriate modulation of Rb1/MyoD transcriptional targets was associated with up-regulation of Rb1, MyoD and their co-activators/repressors transcripts, suggesting a compensatory effort to overcome a molecular block to differentiation at the myoblast/myotube transition during regeneration. This compensation appeared to be effective for MyoD transcriptional targets, although was less effective for Rb1 targets. Analysis of Rb1 phosphorylation states showed prolonged hyper-phosphorylation at key developmental stages in *Emd* null myogenic cells, both *in vivo* and *in vitro.* We also analyzed the same pathways in *Lmna* null muscle, which shows extensive dystrophy. Surprisingly, *Lmna* null muscle did not show the same perturbations to Rb- and MyoD-dependent pathways. We did observe increased transcriptional expression of *Lap2α* and delayed expression of Rb1, which may regulate alternative transcriptional pathways in the *Lmna* null myoblasts. We suggest that the dominant *LMNA* mutations seen in many clinically disparate laminopathies may similarly alter Rb function, with regard to either the timing of exit from the cell cycle or terminal differentiation programs or both.

INTRODUCTION

The muscular dystrophies are a heterogeneous group of over 30 inherited diseases characterized by progressive weakness and degeneration of skeletal muscles. The best characterized of the muscular dystrophies are those involving myofiber cell membrane homeostasis, including appropriate attachment to the basal lamina (dystrophin–dystroglycan-basal lamina) (1,2). Two poorly understood types of muscular dystrophy are the X-linked and autosomal dominant (AD) forms of Emery–Dreifuss muscular dystrophy (EDMD1) (3). These forms of EDMD1 involve components of the nuclear lamina; the X-linked form is caused by emerin deficiency (4), and dominant missense mutations in the *LMNA* gene

*To whom correspondence should be addressed at: Laboratory of Cancer and Developmental Biology, PO Box B, National Cancer Institute, Frederick, MD 21702, USA. Tel: +1 3018461755; Fax: +1 3018467117; Email: stewartc@ncifcrf.gov
†The first three authors contributed equally to the work.

that encodes the A-type lamins result in the AD form of EDMD (5). Both forms of EDMD are clinically distinct from other muscular dystrophies, showing syndromic features of early-onset tendon contractures and cardiac conduction block often requiring implantation of a pace-maker (6).

The pathogenesis of EDMD is particularly intriguing for two reasons. First, it is not clear why mutations in these ubiquitously expressed nuclear proteins result in such discrete patterns of tissue involvement (tendons, muscle, cardiac conduction system). Secondly, different missense mutations of *LMNA* cause a wide range of disorders that often do not show muscular dystrophy as part of their clinical phenotype (7). At least nine congenital diseases, the laminopathies, have been linked to different mutations in the *LMNA* gene that encodes lamins A and C (8,9).

Emerin is an integral protein of the inner nuclear membrane and is ubiquitously expressed in both mitotically active and terminally differentiated (post-mitotic) cells (10). The function of emerin is unclear, although it binds to a variety of other nuclear factors including transcription repressors, an mRNA splicing regulator and barrier-to-autointegration factor (BAF) and a conserved chromatin- and DNA-binding protein (11). Emerin bears structural homology to other lamin-associated proteins, such as LAP2 and MAN1, through a shared LEM domain (12). LAP2 exists as a variety of alternatively spliced isoforms, with each isoform containing the ~40 residue LEM domain that binds BAF. The LEM domain is also found in at least four other proteins including emerin and MAN1 (13).

The lamins, consisting of lamins A, B1, B2 and C, as well as some minor forms, are intermediate filament proteins found in mammalian nuclei. The B-type lamins (lamins B1 and B2) are constitutively expressed. In contrast, A-type lamin (lamins A and C) expression is developmentally regulated, with the A-type lamins being absent from many embryonic and adult stem cells (7,14). Together, the A- and B-type lamins, emerin, LAPs and other proteins form a proteinaceous meshwork, the nuclear lamina, which underlies the inner nuclear membrane. The functions of the lamina include maintenance of the physical architecture and mechanical strength of the nucleus, as well as providing a scaffold with which a variety of other nuclear proteins, involved in DNA replication, chromatin organization and transcription, are associated (15).

The X-linked form of EDMD (EDMD1) is caused by either loss-of-function mutations or deletion of the *EMD* gene (4). The AD form of EDMD (EDMD2) arises because of missense mutations in the A-type lamins that generally disrupt assembly of the lamins into the lamina and affect nuclear morphology (16,17). Some *LMNA* mutations result in a redistribution of emerin from the nucleus to the endoplasmic reticulum and others affect the recruitment of emerin to the nuclear envelope, revealing that the A-type lamins are required for the selective retention of emerin to the nuclear envelope (18). We previously described a mouse line with complete loss of A-type lamin expression in which some features of EDMD2 were present (18,19). The *Lmna*−/− mice were indistinguishable from their normal sibs at birth; however, all *Lmna* null mice were dead by 6–8 weeks. Death was associated with muscle loss and dilated cardiomyopathy (20). EDMD1 and EDMD2 may therefore both arise because of reduced emerin recruitment to the nuclear envelope.

Two recent reports suggested that cell mitosis and differentiation pathways involving the retinoblastoma protein (Rb1) may be involved in the pathogenesis of EDMD1 and other laminopathies. The first showed that Rb protein is destabilized in *Lmna*−/− fibroblasts derived from the *Lmna*−/− mice (21). This was consistent with biochemical data showing physical association of *Lmna* with Rb1 and some forms of LAP2 (22). A recent study of a large series of human muscle biopsies by mRNA profiling showed that key components of the Rb transcriptional regulatory pathway were specifically altered in patients with EDMD1. These authors proposed a model of abnormal myogenesis during muscle regeneration in EDMD1, where the failure of Rb1 to associate with the nuclear lamina results in downstream effects on the timing and/or control of myogenic differentiation. The data supporting this model were from the EDMD1-specific over-expression of proteins involved in acetylation of Rb1 and MyoD (CREBBP, EP300 and CRI-1) and a protein involved in the removal of acetylated histones from activated chromatin (NAP1L1). The hypothesis was that these Rb1/MyoD pathway members showed compensatory up-regulation to overcome a molecular block in downstream transcription pathways (23).

Rb1 is critical for muscle development. *Rb1*−/− mouse embryos die at mid-gestation, showing increased cell death in cells normally expressing Rb, including skeletal muscle precursor cells (24,25). *Rb1*−/− myoblasts show increased cell death prior to myoblast fusion, shorter myotubes with fewer myofibrils, reduced muscle fiber formation, accumulation of elongated nuclei that actively synthesize DNA within the myotubes and reduction in expression of the late muscle-specific genes including muscle creatine kinase and MRF4 (25–27). Also, Rb1 is essential for the E2F-mediated suppression of proliferative transcription programs and exit of myoblasts from the cell cycle (28), as well as serving as an activator of MyoD in promoting the induction of the myogenic transcription program through the transfer of a key acetylase (CREBBP) (29–31).

Here, we describe the derivation of a mouse line that does not express emerin (*Emd* null mice). Although *Emd* null mice show no overt phenotype, we show that Rb1 and MyoD expression levels and pathways regulated by the two factors during muscle regeneration are disrupted and that this disruption is associated with a temporal delay in the rate of muscle regeneration in the *Emd* null mice. Using an *in vivo* muscle degeneration/regeneration model, in addition to the *in vitro* differentiation of primary myoblast cultures, we provide evidence for temporal abnormalities in gene expression and synchronization of the two differentiation pathways at a key timepoint during muscle regeneration. Specifically, we find inappropriate phosphorylation of Rb1 coincides with a temporal failure to both, transcriptionally represses mitotic transcriptional programs via the Rb1/E2F pathway and delays induction of myogenesis genes via the Rb1/MyoD pathway. In contrast, the *Lmna* null mice did not exhibit changes in the levels of the majority of genes that were disrupted in the *Emd* null mice, with the possible exception of *Lap2α* and *Rb1*. Our data suggest that disorders to the

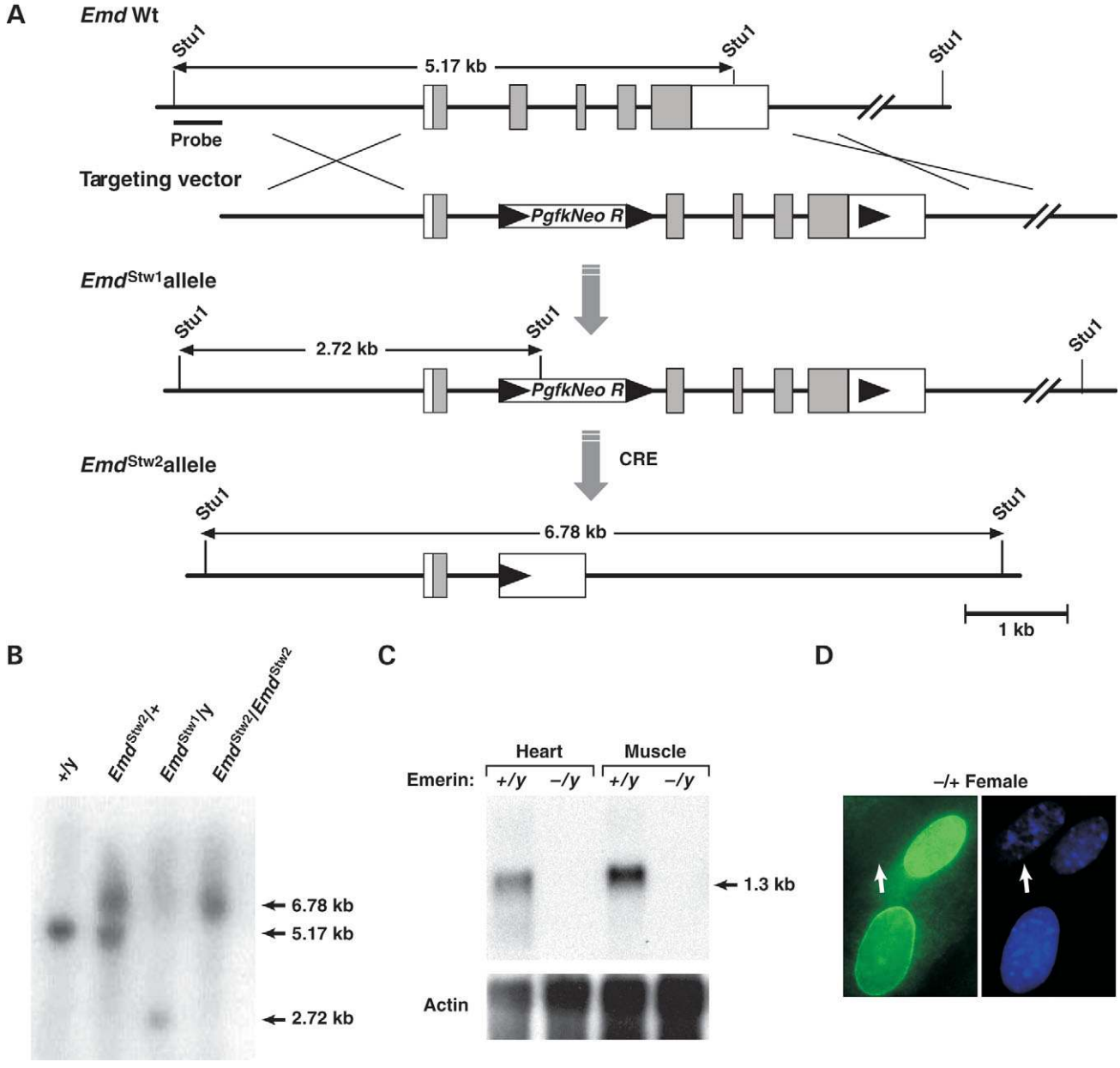

Figure 1. Generation of *Emd* null mice. (**A**) The construction of the targeting vector for deriving a conditional null of the *Emd* gene is shown. A conditional knock-out strategy was used, with crosses to *Cre* recombinase-expressing mice leading to a deletion of four of the five exons of the *Emd* gene. (**B**) Appropriate recombinant loci were confirmed by Southern blot analyses. (**C**) Loss of *Emd* mRNA was also confirmed by northern blot and by immunostaining of nuclei in fibroblasts from heterozygous female carriers. (**D**) DAPI staining shows equal staining of three cell nuclei (right panel) and immunostaining shows two of the nuclei expressing emerin, whereas one nucleus showed no expression (arrow left panel). The somatic mosaicism for emerin expression in females is expected on the basis of X-inactivation.

nuclear lamina may result in inefficient responses to differentiation cues at the timepoint when cells must exit from the cell cycle and start to differentiate terminally.

RESULTS

Derivation of emerin-deficient mice

EDMD1 is caused by mutations in the X-linked *EMD* gene, with most mutations resulting in the complete absence of emerin protein in all cell types. As in humans, murine *Emd* is also X-linked. We generated a conditional floxed allele of *Emd* as shown in Figure 1A. Homologous clones were identified and used to derive germline chimeras that transmitted the targeted allele to their offspring. Heterozygous females or hemizygous males were then crossed with a general *Cre* deletor line of mice (*Rosa26*), which resulted in the deletion of exons 2–6 in the *Emd* gene as shown by Southern blot (Fig. 1B). Complete ablation of the *Emd* gene in the resulting offspring was verified by northern analysis (Fig. 1C), and this

was confirmed by western and immunofluorescent analysis of nuclei from both hemizygous null males and heterozygous females. In heterozygous females, somatic mosaicism for emerin was shown as expected, on the basis of X-inactivation (Fig. 1D).

The nuclear morphologies of the *Emd*−/− and −/*Y* fibroblasts were overtly normal in contrast to *Lmna*−/− nuclei or nuclei expressing some of the laminopathy mutations which show characteristic morphological changes such as herniations and blebbing of the nuclear envelopes, accompanied by a redistribution of other nuclear envelope-associated proteins (18). In *Emd*−/*Y* nuclei, the distribution of other nuclear envelope proteins such as Lap2β or the nuclear pore complexes appeared to be unaffected (data not shown). Although immunostaining for the A-type lamins appeared to be more intense in some of the *Emd*−/*Y* fibroblasts than in the wild-type cells, indicating a possible effect of emerin loss on A-type lamin expression, lamin A transcription or protein levels were not increased in the *Emd*−/*Y* fibroblast nuclei, as determined by western blot and real-time PCR (data not shown).

Emd−/*Y* males and −/− females were overtly normal at birth, and their subsequent postnatal growth, behavior, reproduction and locomotion were indistinguishable from their wild-type siblings. Histological analysis of their tissues revealed no overt pathology or any indication of muscle atrophy, dystrophy or any cardiac pathology, even in relatively old mice (∼1 year). Cardiac function in *Emd*−/*Y* mice, including isoproterenol-induced stress, as measured by ECG analysis, was also normal (data not shown).

Mice lacking the A-type lamins show extensive degeneration and dystrophy in various muscle groups, particularly pharyngeal, tongue, pelvic girdle and perivertebral muscle groups (18). Although the *Emd*−/− and −/*Y* mice showed no overt indications of muscular dystrophy, recent results revealed that many components of a molecular pathway involving *LMNA*, *RB1* and *MYOD* showed similar dysregulation in patients with EDMD1 (*EMD* mutations) and EDMD2 (*LMNA* mutations) (23). We, therefore, asked whether similar perturbations to the myoblast/myotube transcription pathways were present in muscles undergoing regeneration in the *Emd*−/*Y* mice using previously established procedures (32,33). Cardiotoxin (Ctx) was injected into both gastrocnemius muscles of 12–16 week *Emd*−/*Y*- deficient mice, using a 10-needle manifold covering 1 cm^2 Age- and sex-matched normal controls, as well as *Lmna*−/− mice (with appropriate controls) were treated in parallel. From each genotype of mice, six gastrocnemius muscles were treated and examined histologically for three successive timepoints (days 0, 3 and 4 after Ctx injection), making a total of 54 muscles analyzed. Three muscles from each group were selected, which showed the most homogeneous and widespread regeneration pattern and these were mRNA-profiled using Affymetrix murine genome MOE430 2.0 microarrays (27 arrays total). In parallel to these *in vivo* assays, we also looked for perturbations to the *Rb* and *MyoD* pathways at successive timepoints in primary cultures of differentiating *Lmna*−/− and *Emd/Y* myoblasts.

Microarray analysis of regenerating muscle reveals perturbations to molecular pathways upstream of Rb/MyoD

Results from the human expression profiling of EDMD1 and EDMD2 dystrophic muscles revealed that components of the RB1/MyoD pathway were up-regulated in their expression. Furthermore, it was suggested that up-regulation in expression was an attempt, by the regenerating myoblasts, to compensate for a molecular block in the expression/function of the downstream targets of the RB/myocription factors (23). We studied the same pathways in the regenerating muscle of the *Emd*−/*Y* mice. The data were analyzed using two complementary statistical methods. Samples were normalized to time 0 of the normal control, or each individual mouse was normalized to their own time 0. The former shows possible inter-strain differences at the baseline (time 0), whereas the latter will show changes within each individual. Statistical comparisons were done on the third day of regeneration in the mutant lines of mice relative to wild-type controls and also using the longitudinal design by comparing intra-strain from day 3 to day 0.

We found that three of four Rb1/MyoD pathway genes identified in the human study, which regulate protein acetylation, showed increased levels of expression on the third day of regeneration [*Crebbp* (*Cbp*), *Nap1L1* and *Cri-1*] in *Emd*−/*Y* but not in *Lmna*−/− muscle relative to the wild-type muscle (Fig. 2A). Furthermore, the data showed the up-regulation to be transient, with the fourth day muscle showing some normalization of expression levels in the *Emd*−/*Y* mice relative to normal controls and *Lmna*−/− mice. For all three transcripts, *Lmna* null mice showed temporal expression profiles similar or identical to the wild-type controls. This suggests that the pathway perturbations caused by *Emd* deficiency are distinct from those caused by *Lmna* deficiency. This would be consistent with both human and mouse genotype/phenotype data, where *Lmna*-deficient mice show a phenotype that is distinct from humans with EDMD2 *LMNA* AD mutations.

As CREB-binding protein (Crebbp) is the key acetylase that is transferred from Rb to MyoD during the myoblast/myotube transition point, we confirmed the up-regulation of *Crebbp* by quantitative RT–PCR (Fig. 2B). *Crebbp* transcripts were strongly induced in *Emd* − /*Y* mice relative to controls (6.4-fold increase, $P = 0.02$) on the third day of regeneration. The *Crebbp* levels normalized by the fourth day, suggesting that up-regulation in the expression of pathway members was successful in overcoming the hypothesized molecular block in Rb/MyoD downstream pathways. Increased Nap111 protein expression in *Emd*−/*Y* muscle on the third day was also shown by western analysis (Fig. 2D), which revealed the enhanced expression of the higher molecular weight activated and the phosphorylated form of Nap111, suggesting persistent and strong activation of this protein (34).

We also analyzed other components of the Rb phosphorylation and MyoD acetylation pathways that showed up-regulation in the human data. These included Rb1, MyoD and Hdac1 (Fig. 2D). Each of these components of the Rb/MyoD transcriptional pathway was strongly induced on the third day, again consistent with a molecular block downstream of this pathway. As a positive control, we also studied

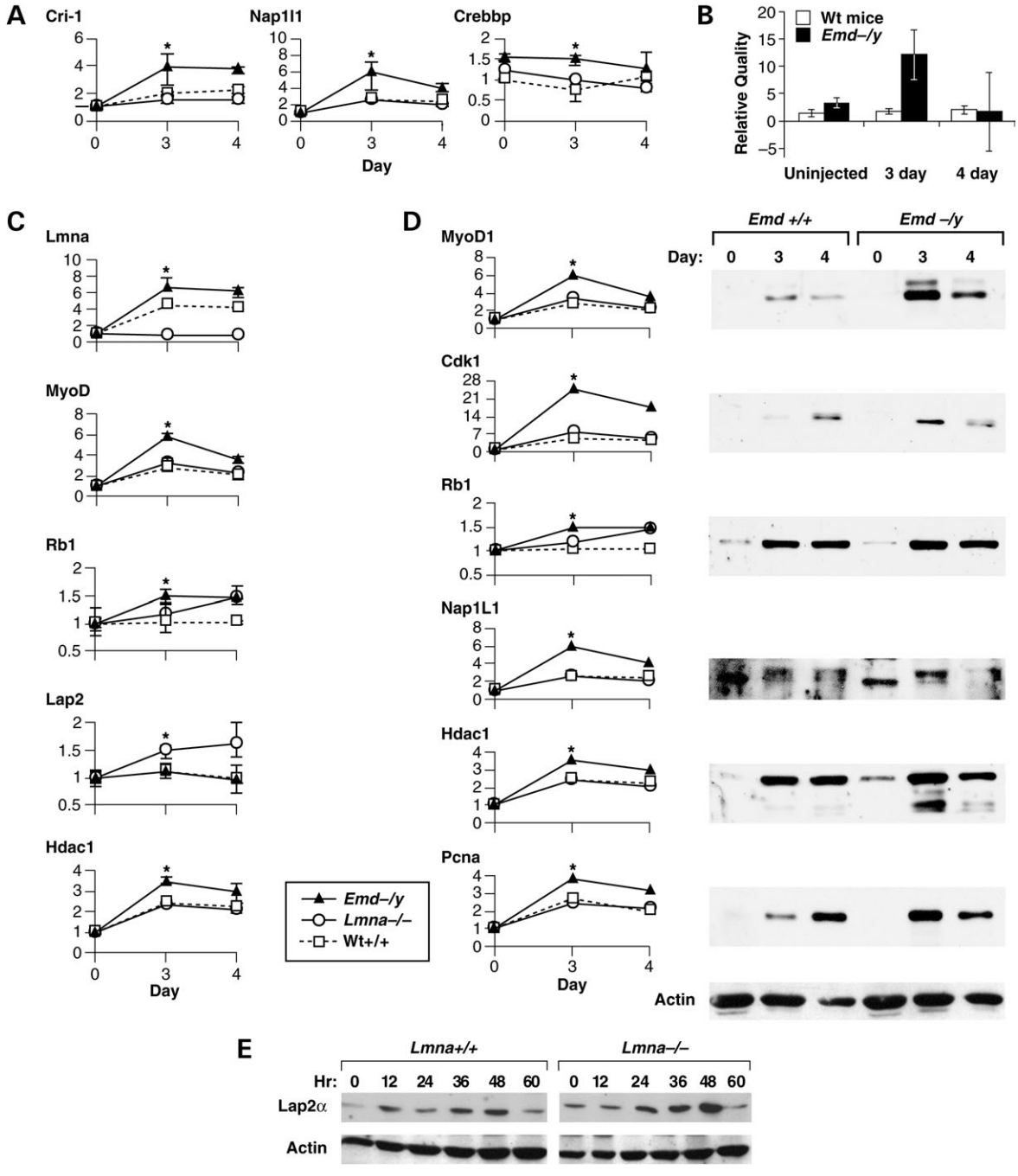

Figure 2. Regenerating *Emd−/Y* muscle shows transient up-regulation of MyoD/Rb1 pathway genes. Analysis of gene expression of MyoD/Rb1 pathway on successive days during *Emd−/Y*, *Lmna−/−* and WT muscle regeneration, with quantification of mRNA transcript levels by oligonucleotide microarray and quantitative RT–PCR. (**A**) Three acetylation/deacetylation members (Cri-1, Nap1L1, Crebbp) identified in human muscle data as specific to EDMD1 showed significant up-regulation at the predicted 3 day timepoint in regenerating *Emd−/Y* muscle (Cri-1 and Nap1L1 are normalized to their own time 0, whereas Crebbp shows normalization to the mean of the three strains at time 0. *Lmna* null mice showed an expression pattern more consistent with wild-type controls. (**B**) Crebbp transcript levels were confirmed using quantitative RT–PCR in different animals at the relevant timepoints. CREBBP showed a 6.4-fold change up-regulation ($P = 0.02$) at 3 days of regeneration in *Emd−/Y* animals. Error bars represent standard deviation. $n = 2$ for wild-type animals; $n = 2$ for *Emd−/Y* animals. (**C**) Microarray analysis for the expression of *Lmna*, *Rb1*, *MyoD*, *Lap2* and *Hdac1* transcripts shows significant up-regulation at day 3 in *Emd−/Y* relative to wild-type muscle. *Lmna* null muscle showed the expected loss of *Lmna* transcripts. *Lmna* null muscle also showed different pattern of Rb1 expression, with increasing expression through 4 days. Significantly, MyoD levels appear to effectively normalize by fourth of regeneration. All values of *Emd−/Y* versus +/+ levels of transcripts were significant at 3 days $P < 0.05$ (*). (**D**) Confirmation of changes in the levels of expression of some of genes identified by array analysis by immunoblotting. Protein from regenerating *Emd−/Y* and wild-type muscle using the indicated antibodies at days 0, 3 and 4 of regeneration. For reference, microarray data for days 0, 3 and 4 is shown to the left of each immunoblot. Increased protein expression for *MyoD1*, *Cdk1*, *Rb1*, *Hdac1* and *Pcna* was observed in *Emd−/Y* at day 3, relative to wild-type muscle. (**E**) In *Lmna−/−* differentiating myoblast cultures, Lap2α levels are transiently increased 48 h after the onset of differentiation levels to the levels seen at the same timepoint in WT myoblast cultures.

Lmna expression. *Lmna* transcripts were absent, as expected, at all timepoints in the *Lmna*−/− mice. However, *Lmna* was slightly up-regulated at all timepoints in the *Emd* mice relative to controls. These results were confirmed at the protein level with MyoD, Cdk1, Nap1l1 and to a lesser extent Rb, showing a marked increase in protein levels on the third day of regeneration or, as for Hdac1, an earlier time in the onset of expression in the *Emd*−/*Y* muscle (Fig. 2D).

In humans, most cases of EDMD2 arise due to AD missense mutations in the *LMNA* gene, although one case was associated with a mutation truncating the lamin A and C proteins at the sixth amino acid, which probably rendered this patient heterozygous for *LMNA* (5). Complete loss of lamin A is not associated with any adult disease and may in fact result in fetal lethality (35). In mice, lamin A/C deficiency is associated with postnatal lethality and muscular dystrophy (18). Despite these differences, we felt that an analysis of degeneration/regeneration in the *Lmna*−/− muscle might also provide supporting evidence for the block of normal-staged Rb1 phosphorylation and MyoD acetylation pathways. We found that Rb1 showed abnormal temporal regulation in the *Lmna*−/− mice, with up-regulation of Rb1 on the fourth day of regeneration in *Lmna*−/− mice, to levels similar to those seen in the *Emd*−/*Y* mice on the fourth day (Fig. 2C). Interestingly, a *Lap2* mRNA isoform showed an increase in expression in the *Lmna*−/− muscle at days 3 and 4 but showed identical levels of expression in the *Emd*−/*Y* and wild-type mice. Subsequent results from the *in vitro* myoblast differentiation of the *Lmna*−/− cells revealed that both *Lap2α* and *Lap2β* are expressed during myotube formation, with *Lap2α* exhibiting a transient increase in expression at 48 h after the onset of differentiation (Fig. 2E). These data suggested that increased expression of *Lap2α* may be compensating for *Lmna* deficiency but not for *Emd* deficiency.

Delayed induction of MyoD-regulated genes, and perturbations to muscle regeneration in *Emd*−/*Y* mice

Data from the analysis of EDMD1 and EDMD2 patients suggested that a relative lag in the induction of MyoD transcriptional targets existed in *Emd*−/*Y* muscle. Transcriptional targets of MyoD, specifically embryonic myosin heavy chain (EmbMHC), myogenesis enhancing factor 2A (Mef2A) and acetylcholine receptor gamma (AChRγ), showed a clear lag in an increase in the levels of expression (Fig. 3A). Wild-type and *Lmna*−/− muscle showed a marked induction at day 3, consistent with the timing of the appearance of MyoD activity. In contrast, *Emd*−/*Y* mice showed no induction at day 3, despite increased levels of MyoD at that same timepoint (Figs 2C and 3A). However, the expression of these markers of MyoD-regulated regeneration was largely normalized by day 4. This suggested that the presumed compensatory increase in the expression of proteins upstream of the MyoD molecular block was eventually effective, allowing the activation of MyoD-regulated genes.

The earlier mentioned mRNA and protein data suggested that the rate of muscle regeneration was altered in *Emd*−/*Y* muscle. To support this, we performed immunostaining on frozen muscle sections from *Emd*−/*Y* and wild-type animals at day 3 and day 7 of muscle regeneration, using antibodies against EmbMHC, a marker of muscle regeneration. Wild-type animals showed that ∼1% of regenerating myotubes tested positive for EmbMHC on the third day (Fig. 3B). In contrast, *Emd*−/*Y* mice showed no detectable EmbMHC-positive cells. These data are consistent with the mRNA profiling, showing a lag in the induction of EmbMHC at day 3 in regenerating *Emd*−/*Y* muscle. At day 7, wild-type mice showed regenerating myofibers of larger size, with clear central nuclei surrounded by cytoplasm/myofibrils that stained variably positive for EmbMHC (Fig. 3B). These regenerating myofibers were relatively homogeneous in size and closely packed. In contrast, the *Emd*−/*Y* muscle on the seventh day showed regenerating myofibers that were on average smaller, more heterogeneous in diameter and separated by endomysial connective tissue. The *Emd*−/*Y* myofibers stained quite variably for EmbMHC, with a subset of the smaller cells staining very intensely for EmbMHC. Indeed, the morphology and staining patterns of a subset of the *Emd*−/*Y* myofibers at 7 days (Fig. 3B, yellow arrows) appeared similar to those of the wild-type mice at 3 days (white arrows). These data are consistent with the reformation of *Emd*−/*Y* myofibers being delayed during muscle regeneration.

We also evaluated the histological outcome of muscle regeneration in the *Emd*−/*Y* and *Lmna*−/− mice at 14 days (*Lmna*−/−) or 17 days (*Emd*−/*Y*) after Ctx injection. By this analysis, there were no obvious differences in the muscle histology from mice of the different genotypes. The percentage of tissue that had regenerated (judged by the presence of central localized nuclei in the myofibers) were similar among *Lmna*−/−, *Emd*−/*Y* and wild-type animals, and fiber diameters were broadly similar, with the exception of some variability in the *Emd*−/*Y* muscle (Fig. 3C). We also saw no indication of fibrosis in the mutant mice. Muscle size of regenerated *Emd*−/*Y* and *Emd*+/+ gastrocnemii appeared to be similar; however, muscle size in *Lmna*−/− and *Lmna*+/+ could not be compared because of significant differences between the body sizes of the mutant and wild-type mice at this age.

Emd−/*Y* muscle, therefore, shows an excess of MyoD and associated transcriptional components at day 3, but also an apparent failure of increased MyoD levels to act upon a subset of its transcriptional targets at this same timepoint. These data are consistent with a temporal molecular block affecting MyoD action during the regeneration of *Emd*−/*Y* muscle.

Analysis of the Rb1/E2F pathway shows inappropriate suppression target gene expression during muscle regeneration in *Emd*−/*Y* mice

During exit from the cell cycle, Rb1 has well-described roles in regulating histone de-acetylation and methylation, largely through the actions of a series of downstream target genes, where it plays a repressive role together with the E2F transcription factors. We expected that alternations in Rb1 phosphorylation state and/or its recruitment of Hdac1 from MyoD would lead to inappropriate and persistent expression of E2F transcriptional targets and changes in the timing of cell cycle withdrawal and terminal differentiation.

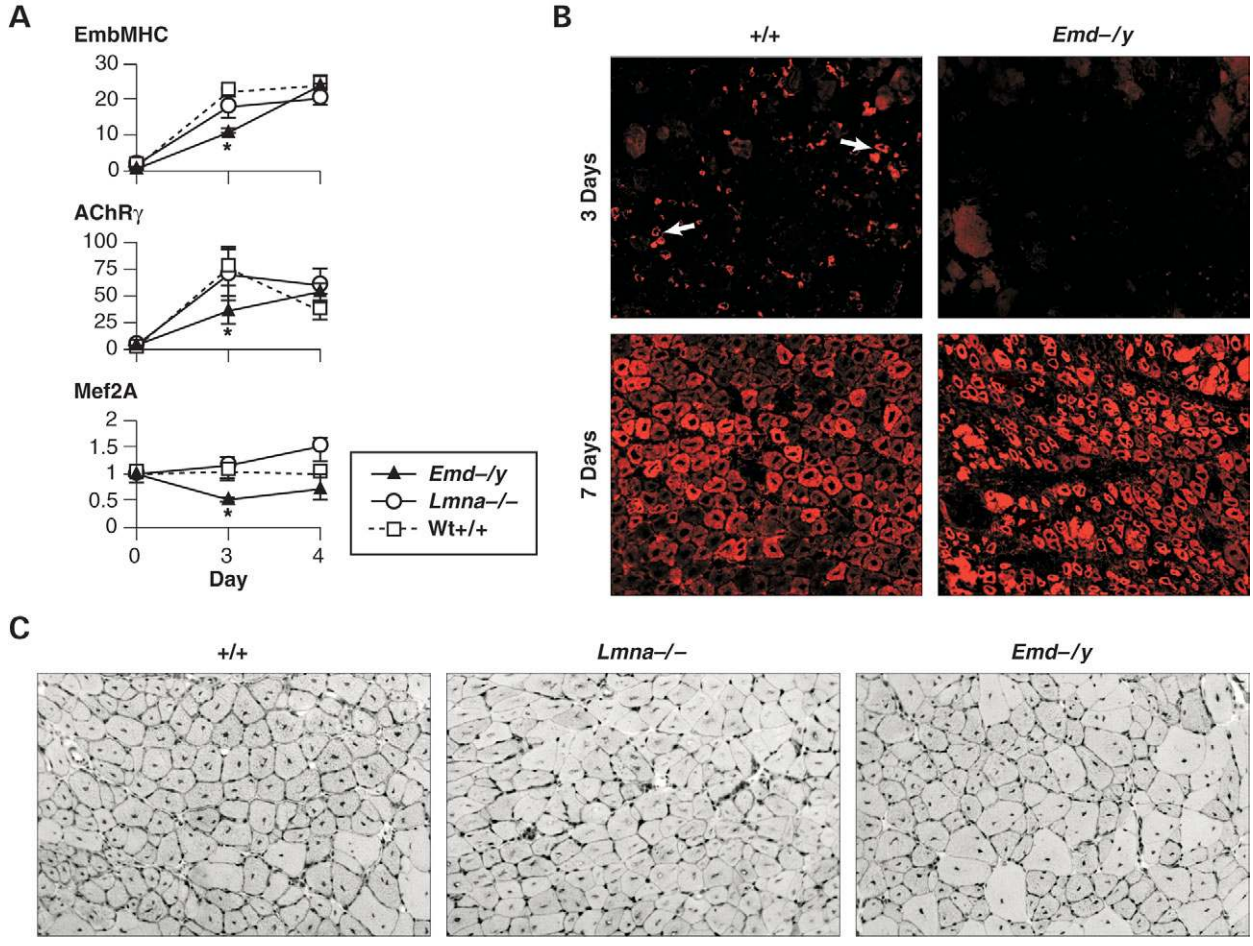

Figure 3. Transcriptional targets of MyoD show delayed induction, despite an increase in abundance of MyoD transcriptional machinery. (**A**) Three downstream transcriptional targets of acetylated MyoD show significantly reduced levels of transcripts in *Emd−/Y* muscle at day 3 of regeneration. This lag in induction of MyoD transcriptional targets occurs despite the strong over-expression of the MyoD transcriptional machinery at this same timepoint (Fig. 2C and D). In each case, expression appears to recover within 24 h, indicating a transient block in downstream target induction. All values of *Emd−/Y* versus +/+ levels of transcripts were significant at 3 days $P < 0.05$ (*). (**B**) Immunostaining of a MyoD-regulated gene, EmbMHC at 3 and 7 days, regenerating muscle from wild-type (+/+) and *Emd−/Y* mice. WT muscle shows induction of EmbMHC in a subset of small regenerating myotubes at day 3, commensurate with induction of MyoD (upper left panel; white arrows). No EmbMHC positive myotubes are seen in *Emd−/Y* muscle at the same timepoint (upper right panel). By 7 days, wild-type muscle shows regenerating myofibers of homogeneous size with central nuclei (dark central cores), with EmbMHC beginning to decrease in expression as the cells mature (lower left panel). *Emd−/Y* muscle at 7 days show smaller and more heterogeneous myotubes and myofibers, with some regenerating myotubes appearing similar to wild-type 3 day cells (yellow arrows). *Emd−/Y* cells show much more variable expression of EmbMHC and fiber diameter consistent with poorly staged induction of MyoD-regulated transcripts. (**C**) By day 14 of regeneration, muscle has reformed in all three genotypes. Fiber diameters were broadly uniform in the WT and *Lmna−/−* muscle, and in *Emd−/Y* muscle, there was some variability in fiber diameter.

We identified Rb downstream target genes by interrogation of well-documented pathways, as well as more recent mRNA profiling (36–38). Rb downstream targets DNA ligase 1 (*Lig1*), polymerase delta (*Pold*), ubiquitin-conjugating enzyme E2 C (*Ube2c*), thymidine kinase 1 (*Tk1*), proliferating cell nuclear antigen (*Pcna*), *Cdc2A*, Cyclin B2, ribonucleoside-diphosphate reductase M2 (*Rrm2*), high-mobility group box 2 (*Hmbg2*), DNA replication licensing factors (*Mcm3, Mcm6, Mcm7*) and S-phase kinase-associated protein 2 (*Skp2*) all showed increased transcript levels specifically in *Emd−/Y* but not the *Lmna−/−* muscle, indicative of a failure of Rb1 repression (Fig. 4).

In both cycling and terminally differentiating muscle, Rb1 repression is mediated by the reversible recruitment of histone deacetylases (HDACs) to gene promoters (39,40). In cells permanently exiting from the cell cycle, S-phase genes are permanently repressed through methylation by a mechanism that involves SUV39H-mediated histone H3 lysine 9 methylation (H3K9) (39) and heterochromatin protein 1 (HP1) recruitment (41–43). Deacetylation by HDACs seems to be a necessary step preceding methylation, as Suv39h1 cannot methylate acetylated histones (42). Other enzymes that have been implicated in Rb-mediated repression are BRG1/BRM (SWI/SNF chromatin remodeling enzymes) (44) and DNA methylase1 (45). We found that Hdac1 and Hp1a were all up-regulated on the third day in *Emd−/Y* muscle when compared with *Lmna+/+* and *Lmna−/−* animals (Fig. 4), consistent with a possible block in the Rb-mediated gene repression. Despite the significantly increased levels of Rb1 and Rb-co-regulators in *Emd−/Y* mice, the transcriptional

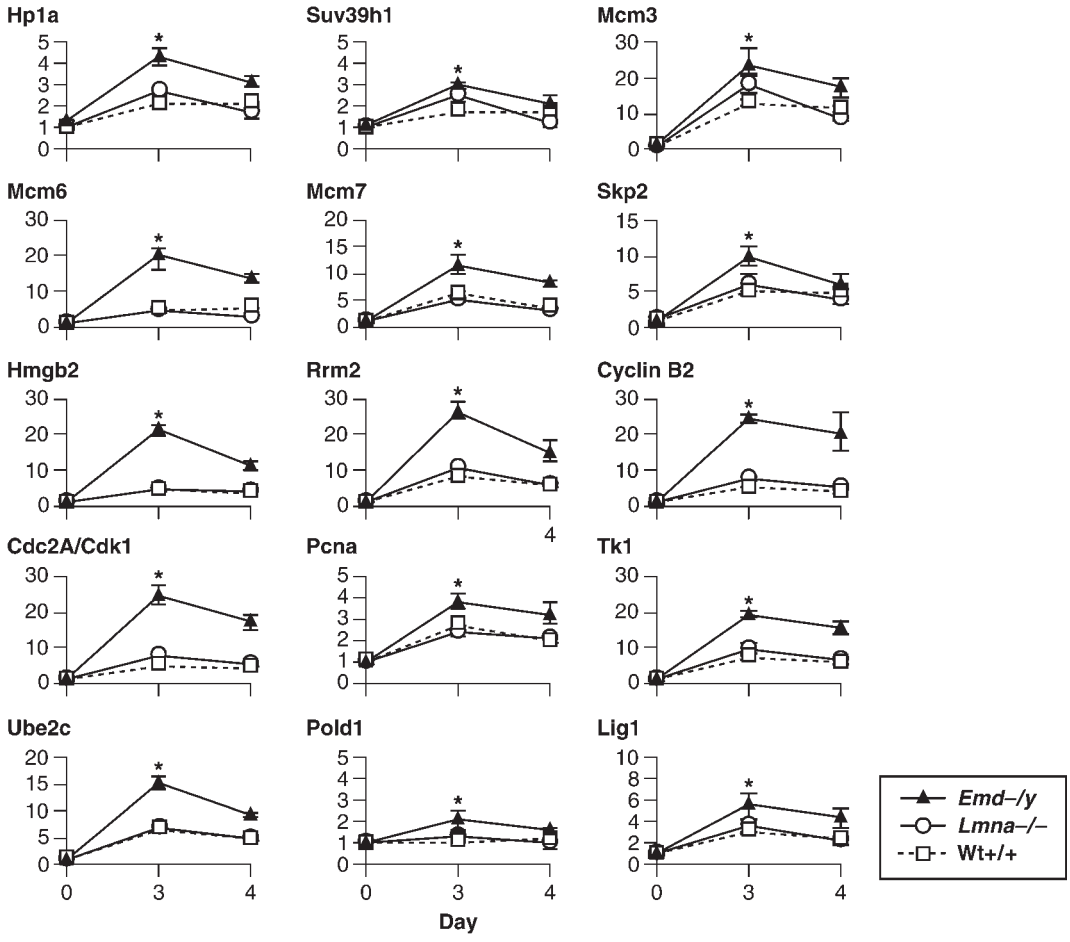

Figure 4. E2F transcriptional targets regulated by Rb1 show up-regulation in regenerating *Emd−/Y* muscle. A series of known targets of the Rb1/E2F pathway were analyzed in mRNA profiles from regenerating in +/+, *Emd−/Y* and *Lmna−/−* muscle. All microarrays were normalized to time 0 for each strain. Components of the E2F complex showed increased levels of corresponding transcripts HP1a; Suv39H, as well as Hdac1 and Rb1 (Fig. 3A) in the *Emd−/Y* samples. In addition, all transcriptional targets of the Rb1/E2F pathway showed a relative failure of transcriptional repression (Mcm3, Mcm6, Mcm7, Skp2, Hmgb2, Rrm2, Cyclin B2, Cdc2A/Cdk1, Pcna, Tk1, Ube2C, Pold1, Lig1) at the same timepoint. These data are consistent with a relative failure of the Rb1/E2F complex to repress target gene expression in the *Emd − /Y* regenerating muscle. All values of *Emd−/Y* versus +/+ levels of transcripts were significant at 3 days $P < 0.05$ (*).

targets of this pathway showed a temporal failure in Rb1-mediated repression (Fig. 4).

The timing of Rb phosphorylation in regenerating muscle is altered by loss of emerin and A-type lamins

Previous reports suggested a direct association between Rb1 and the A-type lamins and that this association is dependent on the phosphorylation status of Rb (21,22). We hypothesized that emerin is also involved in the Rb/lamin association, and thus emerin loss-of-function may indirectly alter the phosphorylation status of Rb. To test this, protein extracts from regenerating muscle at different timepoints from wild-type, *Lmna−/−* and *Emd−/Y* mice were tested for Rb1 levels and phosphorylation status (mobility shift) by western analysis (Fig. 5A). By this analysis, we found that wild-type animals expressed Rb and hyper-phosphorylated forms of Rb (ppRb) by the third day of regeneration, consistent with temporal expression profiling in normal regeneration. The ppRb1 protein appeared short lived, with the majority of both Rb and ppRb being lost by the fourth day of regeneration (Fig. 5A). *Emd−/Y* muscle showed normal induction of Rb and ppRb at 3 days; however, the hyper-phosphorylated form was abnormally persistent through to the fourth day (Fig. 5). These data are consistent with disrupted post-translational modifications of Rb, with a relative failure in the timing of dephosphorylation of Rb1 and removal of the protein.

Lmna−/− mice showed a distinct pattern, where basal levels of Rb1 in normal muscle appeared elevated, but the induction of phosphorylated forms was delayed relative to both normal and emerin-deficient mice (Fig. 5A).

In vitro differentiation of *Emd−/Y* myoblasts is delayed and shows altered regulation of Rb phosphorylation

We also investigated whether the establishment and differentiation of primary myoblasts cultures were affected by loss of emerin. Primary myoblast cultures from the fore- and hind-limb musculature of wild-type and *Emd−/Y* mice were established

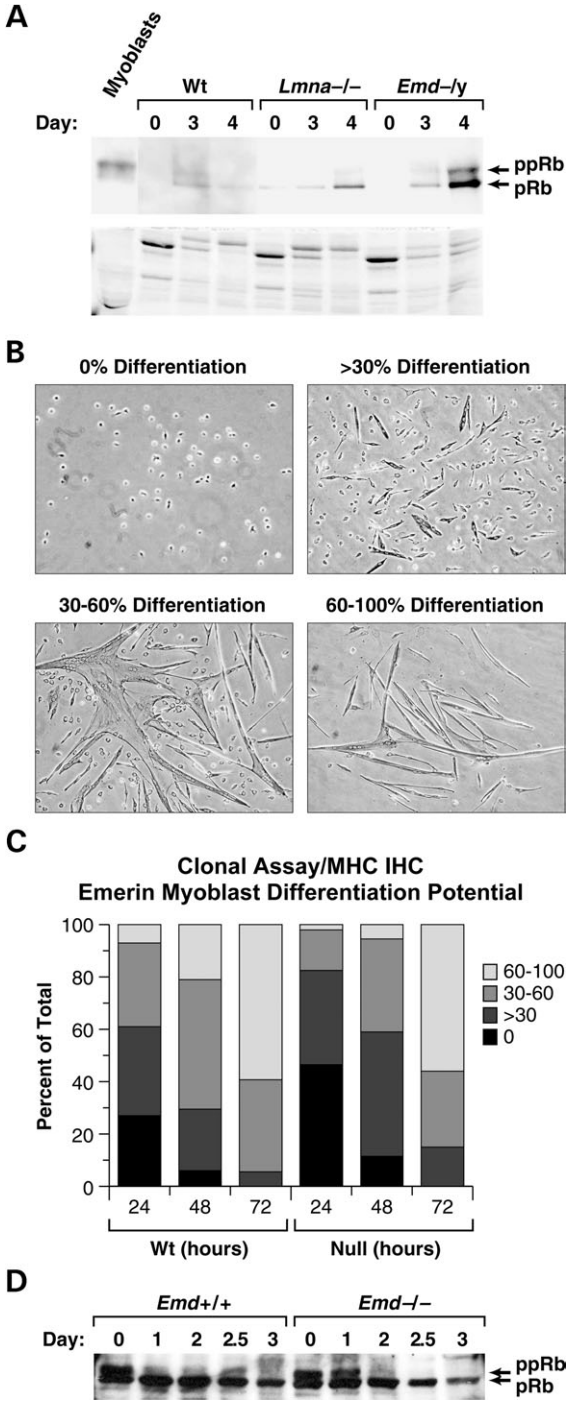

and induced to differentiate into multinucleated myotubes by withdrawal of basic fibroblast growth factor (bFgf) and a reduction in serum concentration. As with the regenerating *Emd−/Y* muscle, *in vitro* differentiation of the *Emd−/Y* myoblasts showed levels of ppRb were prolonged when compared with the levels in +/+ myoblast differentiation during the first 24 h after the onset of differentiation (Fig. 5B)

A comparison of the numbers of individual myoblast clones that started to form myotubes (reviewed in 46) revealed a significant difference in the onset differentiation between the +/+ and mutant myoblasts. Of the +/+ myoblast clones, 72% showed myotube formation within 24 h after the onset of differentiation, whereas only 52% *Emd−/Y* myoblast clones were forming myotubes within the first 24 h (Fig. 5C). *Emd−/Y* myoblasts, therefore, showed a delay in the onset myotube formation. By 48 h, the differences between *Emd−/Y* and +/+ clones were indistinguishable, with both genotypes showing 90–95% clones forming myotubes (Fig. 5D). These results were comparable to the initial delay and later to the recovery in myotube differentiation seen *in vivo*. No significant differences in the rate of *in vitro* myotube formation were seen with the same culture system performed on the *Lmna−/−* myoblasts (data not shown).

DISCUSSION

Here, we describe, by targeted deletion of the X-linked gene, *Emd*, the derivation of a mouse line that does not express emerin. We derived this line to generate a mouse model for EDMD1 that is caused by loss-of-function mutations in the *EMD* gene. In EDMD1 patients, muscle wasting does not usually start until adolescence. Furthermore, EDMD1 muscle is not dystrophic i.e. the muscle fibers do not show degeneration, although there is variation in fiber diameter, with some fibers having centrally localized nuclei. Patients develop cardiac conduction abnormalities, which often require the fitting of a pacemaker and defibrillator to avoid a potentially fatal dysarrhythmia (47). Despite genetic and molecular similarities of our mice to emerin-deficient EDMD1 patients, hemizygous and homozygous null mice showed no overt histopathology or cardiac symptoms up to and beyond 1 year of age. In addition, a more sensitive analysis on isolated cardiomyocytes from the *Edmd1* mice suggested the presence of defects in myocyte contractility; however, these results were too inconsistent to arrive at any firm conclusion (W. Giles, personal communication).

Figure 5. The staged timing of Rb phosphorylation states is altered in regenerating *Emd−/Y* muscle. (**A**) Western analysis of Rb1 from proliferating C2C12 myoblasts and muscle homogenates from regenerating muscle at successive timepoints from the indicated mouse strains (top panel). The lower panel shows total protein staining of the filter, as a control for loading in each lane. Proliferating myoblasts show hyper-phosphorylated ppRb as the predominant form of Rb (higher molecular weight bands). *In vivo* in +/+ muscle (WT), Rb1 is transcriptionally induced on day 3 of regeneration, where both hypo-phosphorylated (pRb1) and hyper-phosphorylated (ppRb) forms of the protein are at approximately equal levels. *Emd−*/Y muscle shows significantly increased levels of both pRb and ppRb at day 4, despite the failure to repress E2F transcriptional targets (Fig. 4). *Lmna−/−* muscle shows increased basal levels of pRb at day 0 and a persistence of both pRb and ppRb at day 4. The lower panel shows the Coomassie-stained protein gel as a loading control.(**B**) Cultured *Emd−*/Y primary myoblasts showed delayed myotube formation and prolonged ppRb phosphorylation. The photos show representative stages of clonal myoblast formation of myotubes. (**C**). The percentage of clones showing different levels of myotube formation at different timepoints during differentiation reveals that during the first 2 h >80% of the *Emd−/Y* myoblasts had not started to form myotubes or showed minimal differentiation when compared with +/+ myoblasts in which only 60% contained no or only a few myotubes. However, by 72 h, the numbers of myotube containing colonies that showed >60% myotube formation was indistinguishable between the +/+ and *Emd−/Y* cultures ($P < 0.1$). (**D**). Differentiating *Emd−/Y* myoblasts show persisting high levels of ppRb and pRb1 1 day after the induction of differentiation, which do not decline until after 2 days of differentiation. In +/+ cultures, PPRb1 levels had declined after day 1 of differentiation.

It is not unusual for mouse models to show a milder phenotype than the corresponding human disease, and this lack of phenotype is often attributed to functional redundancy with other proteins and/or strain differences. However, the nature of the functional redundancy is rarely defined. Here, using a staged *in vivo* and *in vitro* muscle regeneration model in these mice, we were able to uncover perturbations to key molecular pathways during muscle regeneration and identified possible compensatory mechanisms the cells use to overcome these molecular perturbations.

A recent bioinformatic analysis of muscle biopsies from patients with either EDMD1 or EDMD2 showed that these two dystrophies have very similar gene expression profiles, with both EDMD dystrophies being only distantly related to most other types of muscular dystrophy (23). In that study, the authors proposed a model suggesting that the process of muscle regeneration might be compromised in EDMD1 muscle because a molecular block at the point myoblasts exit from the cell cycle and undergo terminal differentiation. We thus investigated whether induction of muscle regeneration in *Emd* null mice would reveal at least a part of the molecular phenotype underlying EDMD in humans. Our results support the suggestion that the Rb1/MyoD pathway is disrupted in *Emd* null mice and that disruption of these pathways is associated with a noticeable delay in the rate of muscle regeneration and myotube formation.

The Rb1 and MyoD proteins are major factors regulating muscle differentiation. Rb1 recruits a HDAC1 from MyoD, allowing MyoD to become acetylated by Crebbp, and thereafter efficiently transcribe downstream myogenic target genes (48–50). The human muscle biopsy data showed up-regulation of four members that regulate acetylation (CREBBP, CRI-1, NAP1L1 and EP300), suggesting that an increase in expression of these four genes reflected a compensatory response to overcome a block in the acetylation of MyoD (23). If this suggested mechanism is correct, we would expect to see a compensatory increase in gene expression specifically on the third day of regeneration in mice, as well as a failure in the induction of transcriptional targets of MyoD in *Emd* null regenerating muscle. Results from the *Emd* null mice showed that three proteins that regulate acetylation (Crebbp, Cri-1 and Nap1l1) were up-regulated on the third day, as were four members of the MyoD/Rb1 complex, which included *MyoD, Rb1, Lmna* and *Hdac1* (Fig. 2C). In support of this model, some transcriptional targets of MyoD showed a significant reduction in levels of transcription at the same timepoint, including *Mef2A*, *EmbMHC* and *AChRγ* (Fig. 3A), despite increased levels of MyoD. Immunostaining of regenerating muscle at 7 days showed *Emd* null muscle having a delayed induction of a key myogenic marker *EmbMHC*, as well as morphological evidence for regeneration being poorly coordinated (Fig. 3B).

During regeneration, Rb1 activity is inhibited by hyper-phosphorylation (ppRb). The active, hypo-phosphorylated form of Rb1 serves both to recruit Hdac1 from MyoD and to suppress myoblast proliferation through the E2F pathway (28). Also, the hypo-phosphorylated form of Rb is recruited to interact with Lap2α and lamin C, components of the nuclear lamina (22,51). We determined the phosphorylation state of Rb1 during myogenic differentiation in *Emd−/Y* muscle. *In vivo*, we found that Rb1 was appropriately induced on the third day of regeneration in *Emd−/Y* muscle, but the normal kinetics of dephosphorylating Rb was delayed, leading to increased levels of both hyper- and hypo-phosphorylated forms by the fourth day of regeneration (Fig. 5A). This persistence of ppRb levels implied Rb activity was delayed, inhibiting the onset of myoblast differentiation. These observations were supported by the persistence of ppRb forms in cultured *Emd−/Y* myoblasts, 24 h after the onset of differentiation (Fig. 5C). Therefore, not only were the absolute levels of Rb1 affected by the mutations, Rb1 activity, as inferred from the prolongation of ppRb1 levels, was also affected by alterations to components of the nuclear lamina. Despite the effects of emerin loss on Rb phosphorylation in the *Emd−/Y* muscle, the Rb1/MyoD pathway was up-regulated, and this was effective at inducing the expression of downstream mRNA targets (*EmbMHC, AChRγ*), albeit a day late.

In contrast to the *Emd* null mice, *Lmna*-deficient mice have dystrophic muscle. Despite the *Lmna* null mice being dystrophic, they did not show the same perturbations in expression of the MyoD targets as seen in the *Emd−/Y* muscle. In the *Lmna* null muscle, we found an up-regulation of Rb1 both in day 0 and in day 4 regenerating muscle (Figs 2C and 5A). In addition, an apparent compensatory up-regulation of *Lap2α* was also noted, as Lap2s are required for the recruitment of HDACs and Rb1 to the lamina (51,52). Thus, different compensatory mechanisms may exist between *Lmna* null and *Emd* null regenerating muscle. Our results are also supported by other reports using immortalized C2C12 myoblasts expressing EDMD1 mutant variants of *Lmna*. These studies revealed that the *Lmna* mutants impaired myotube formation, disrupted Lap2α/A-type lamin complexes and resulted in the persistence of hyper-phosphorylated ppRb1 (51,53).

An additional explanation as to why the pathological outcome was different between the *Emd* and *Lmna* null mice is that the loss of emerin is maybe compensated by an up-regulation in lamin A expression in muscle (Fig. 2C). In the *Lmna* null mice, emerin probably cannot compensate for the loss of the lamins, as emerin depends the A-type lamins for its normal localization to the nuclear envelope (18). In addition, loss of the A-type lamins probably increases the susceptibility of the muscle cells to mechanically induced apoptosis. *Lmna−/−* fibroblasts succumb more readily to apoptosis and necrosis when subjected to repetitive mechanical stress, and their nuclei are both weaker and structurally deformed when compared with wild-type nuclei (54). This may be a contributing factor to the *Lmna−/−* phenotype. Emerin-deficient mouse fibroblasts, however, are less prone to mechanically induced apoptosis than lamin-deficient cells but show normal nuclear mechanics. They do, however, show attenuated induction (by mechanical stress), although to a lesser extent, than the lamin-deficient cells of anti-apoptotic gene expression by some unidentified signaling pathway (55). In EDMD1 patients, the muscle pathology may, therefore, arise because of attenuation at inducing anti-apoptotic gene expression together with the perturbations to the Rb1/E2F pathway that delay muscle regeneration. In contrast to EDMD2 patients, the EDMD1 muscle pathology may also

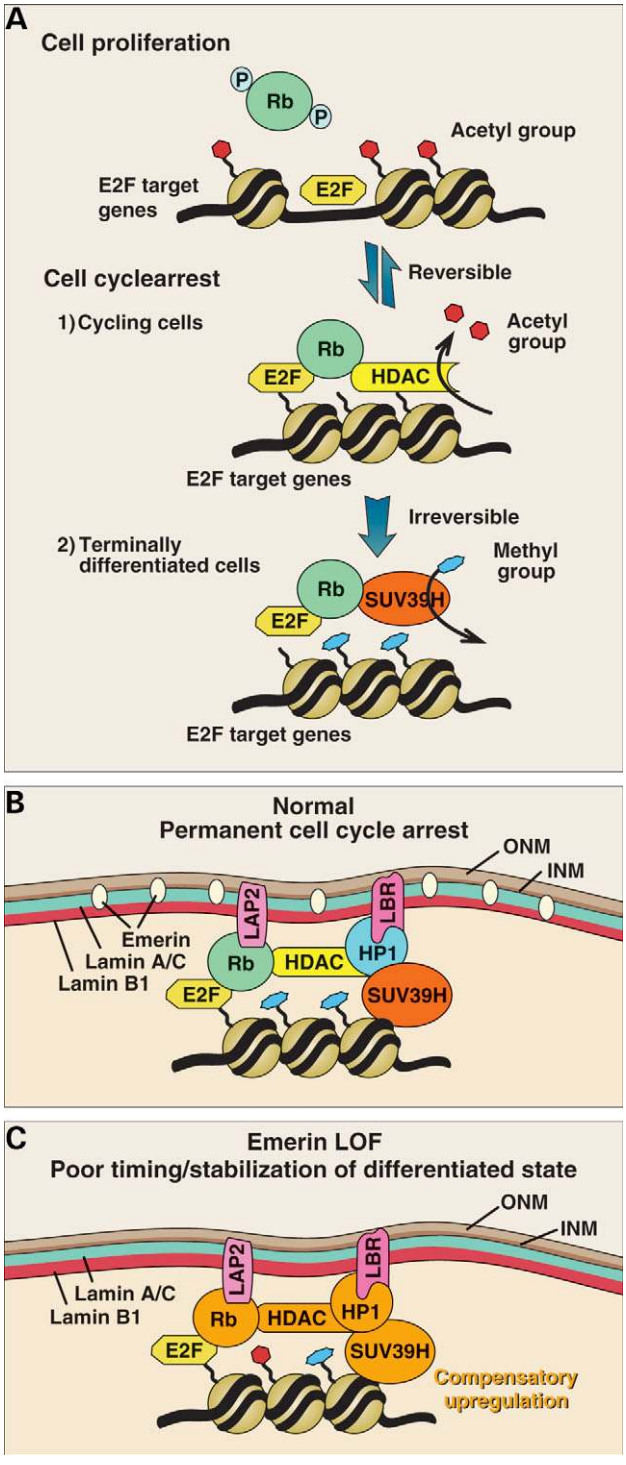

be milder because of a transient up-regulation of A-type lamin expression that compensates for the loss of emerin.

A model for involvement of the nuclear lamina in regulating muscle regeneration

In proliferating cells, the E2F pocket proteins, together with E2F transcriptional targets and their associated acetylated histones drive the cell cycle (56). As cells begin to leave the cell cycle, Rb1 is dephosphorylated and associates with HDACs, with the Rb1/HDAC complex binding the E2F target genes, leading to the deacetylation of histones and transcriptional silencing (57,58) (Fig. 6). This results in cell cycle arrest that is reversible (39,41–43,45). Further commitment to the post-mitotic and differentiated state involves the association of the histone methyltransferase SUV39H with Rb1 and the methylation of histone H3 at lysine 9 by SUV39H. This terminally differentiated state is irreversible (Fig. 6C).

Given these results and the data presented here, we can extend this model to include the nuclear lamina (Fig. 6B and C) as being required for the effective regulation of factors required in muscle regeneration. Dephosphorylated Rb1 binds to the lamins and LAP2α. In addition, HDACs interact with LAP2β at the nuclear envelope where the HDAC/LAP2β complex deacetylates and suppresses expression of a variety of genes (52). Subsequently, the methylation of histone H3 by SUV39H results in the recruitment of HP1, with HP1 binding to the nuclear envelope via the lamin B receptor (LBR) (59). HP1 either stabilizes the RB1/SUV39H complex or protects H3 lysine 9 residues from demethylases. We hypothesize that emerin is required for the stability of the lamin A/C/LAP2/Rb complex and/or the LBR/HP1/SUV39H complex.

In *Emd* null myoblasts, we suggest that these protein complexes are unstable or do not form because of absence of emerin from the nuclear envelope (Fig. 6). Evidence for this comes from the significant up-regulation of most of the members of this complex, including Rb1, Suv39 h, Hdac1 and HP1, at the key timepoint in myoblast differentiation (days 3–4). Despite the up-regulation in the expression of this complex, at this timepoint, most downstream E2F target genes were inappropriately repressed (Fig. 4). Indeed, the failure to repress E2F targets is more widespread, and longer lasting, than seen for MyoD transcriptional targets. As with the Rb1/MyoD pathway, the compensatory increase in expression of the Rb1/E2F pathway was eventually effective, allowing muscle regeneration to proceed. However, the regenerating muscle shows late induction of the differentiated state and poor coordination of regeneration between neighboring

Figure 6. Schematic model of the consequences of emerin and lamin A/C mutations on the downstream function of Rb/E2F pathways. **(A)** A summary of models to alterations to the chromatin structure of E2F target genes, based upon the existing literature. E2F target promoters are transcriptionally active in proliferating cells (top) where E2F transcription machinery to bound to acetylated histones, with Rb being hyper-phosphorylated and unable to bind to E2F. Reversible cell cycle arrest (middle panel) occurs when Rb becomes hypo-phosphorylated, whereupon it recruits Hdacs into the E2F transcriptional complex, resulting in histone de-acetylation. Irreversible exit from the cell cycle (lower panel) occurs with Hdacs, which are replaced by SUV39H, with the histones becoming methylated. (**B**) The proposed participation of the nuclear envelope and lamina with the formation of Rb complexes during exit from the cell cycle. Data presented in this article are consistent with the evidence that LBR1, A-type lamins, emerin and LAP2s directly and indirectly associate with Rb1 and HP1. The transcriptional induction of Lmna by myoblasts as they exit the cell cycle likely facilitates formation of the complex and irreversible exit from the cell cycle. (**C**) The proposed perturbations to the regulation of E2F target genes when emerin is lost from the inner nuclear membrane. Most components of the de-acetylation/methylation complex show significant up-regulation in *Emd*−/*Y* muscle (Rb, HP1, Hdac1, Suv39H), yet the target genes show abnormal high persistence of expression (Fig. 4). The model suggests that signaling downstream of Rb is compromised because of inappropriate protein/protein interactions at the INM and lamina.

cells (Fig. 3B), and by 17 days, such uncoordinated regeneration appears to have been largely rectified.

Our results also document the surprising plasticity myogenic cells show as they overcome a molecular block in their differentiation. The compensatory increase in expression of many pathway members we observed in *Emd* null myogenic cells is noteworthy and may explain the effective regeneration of *Emd* null muscle, as well as the overtly normal phenotype of *Emd* null mice.

One must also question why EDMD1 patients show a more severe disorder, including early-onset contractures and cardiac conduction block when compared with mice. Human and mouse cells show different susceptibilities to apoptosis due to loss of RB function, with many types of human cells displaying a more pronounced apoptotic effect in the absence of RB. Consistent with this, RB is expressed at higher levels and regulates many apoptotic genes in humans, but mouse cells show a significant blunting of the Rb-mediated apoptosis pathways (60). Therefore, a plausible explanation to the absence of a disease phenotype in *Emd* null mice is that more cells are able to contribute to muscle regeneration because fewer cells are lost by apoptosis due to Rb1 dysfunction when compared with humans.

Implications for other laminopathies

This model for muscle regeneration may be extended as a potential model for some of the other laminopathies. Rb1, and the related Rb-like proteins (p130/Rbl-1, p107/Rbl-2) are critical to the differentiation of fat, heart, bone and other cell types (61). It is likely that the induction of differentiation by Rb proteins is coordinated with the shift in nuclear envelope composition in most cells, as we have shown for myogenic cells. An extension of our model is that different missense mutations in *LMNA* may result in abnormal protein/protein interactions at the Rb/E2F complex and similarly disrupt the timing of cell cycle arrest and execution of the differentiated state. Thus, the AD laminopathies may result in gain- or change-of-function mutations affecting cell- and developmentally specific protein/protein interactions centered on the Rb/E2F pathways and/or additional pathways regulating cell proliferation and differentiation during regeneration.

MATERIALS AND METHODS

Mice

The derivation of the *Lmna*-deficient mice is described (18). All mice were maintained in accordance with the procedures outlined in the Guide for the Care and Use of Laboratory Animals. All wild-type mice were (C57BL6XC3H) F1s. Surgical procedures were performed under tribromoethanol (Avertin) anesthesia according to institutional guidelines (NCI-Frederick ACUC Guidelines and Policies). All mice used were between 6 and 10 weeks of age.

Generation of emerin-deficient ES cells and mice

The *Emerin* cDNA fragment corresponding to 1364–1837 bp was used to screen a 129/SvJ mouse phage library (Clontech). One of these phages containing the genomic sequences of *Emd* matching exon 4 through 4 kb past the last exon was used to produce a replacement targeting vector containing *PGKneo* and *TK* cassettes. A conditional floxed allele of *Emd* was derived by introducing a floxed Pgk*Neo* selectable marker in the first intron and an orphan *LoxP* cassette in the 3′-untranslated region of the *Emd* gene. The *TK* cassette was introduced in the *Not*I site of the *Nhe*I fragment. This final construct was used for the electroporation of the W9.5 embryonic stem (ES) cells (62). ES clones heterozygous for the mutated allele were derived and two independent lines of mice (nos 17 and 20) were derived by C57Bl/6 blastocyst injection. Both lines showed the same expression characteristics. *Emd*-deficient mice were derived from crosses between the *Emd* mice, with mice transgenic for the ubiquitously expressed b-actin-Cre (63).

Northern blotting

Total RNA from different tissues of wild-type and/or *Emd*-deficient mice were obtained using the RNAeasy system (Qiagen). Four to six mice were used to provide a particular tissue or tissues from any particular timepoint. A total of 10 mg of each sample were loaded per slot onto a formaldehyde 1% agarose gel. The RNA was transferred to Hybond-N+ membranes (Amersham Pharmacia) and hybridized with 32P labelled cDNA probes using ExpressHyb hybridization solution (Clontech) following the manufacturer's instructions.

Primary myoblast isolation/proliferation protocol

Myoblasts were excised from fore-limbs and hind-limbs of 5–6-week-old *Lmna*−/− and *Emd* null mice, as well as age-matched controls. The limbs were rinsed in a solution of 2% Penn/Strep/1 μg/ml fungizone/PBS. Muscle tissue was isolated from bone and digested using 4 ml digestion buffer/gram of tissue for 2 × 15 min incubations at 37°C. The digestion buffer consisted of a 1 vol Dispase II (Roche cat. no. 295 825): 1 vol 1% Collagenase II (Gibco cat. no. 17101-015) with 2.5 mM $CaCl_2$. Between 15 min incubations, the tissue was titrated with a 5 ml pipette to enhance the isolation of myoblasts. An equal volume of DMEM 10% FBS [DMEM (Specialty Media cat. no. SLM020-A), 10% FBS (Hyclone), 50 IU/ml penicillin/50 μg/ml streptomycin (Gibco cat. no. 15140-122)] was added to the cell suspension and consecutively filtered through a 40 and 70 μM filter. The cells were centrifuged for 5 min at 12 000 r.p.m. and washed twice with DMEM 10% FBS. The cell pellet was resuspended in 10 ml of DMEM 10% FBS and pre-plated on 150 mm tissue culture dishes for 1–2 h at 37°C/5%CO_2 to allow fibroblasts to adhere to the dish. The non-adherent cells, enriched for myoblasts, were then harvested and plated onto 100 mm gelatin (Sigma cat. no. G-2625) coated tissue culture dishes in growth media consisting of Hams F-10 (Gibco cat. no. 11550-043), 20% horse serum, 1.26 mM $CaCl_2$, 50 μg/ml gentamycin (Gibco cat. no. 15750-060), 50 IU/ml penicillin/50 μg/ml streptomycin (Gibco cat. no. 15140-122), 0.8 μg/ml Fungizone (Gibco cat. no. 15290-018) and 10 ng/ml

bFGF (R and D systems). Proliferating myoblasts were re-fed daily with fresh growth media.

Primary myoblast differentiation and clonal analysis

Primary myoblasts were plated onto $6 \times 100\ mm^2$ gelatin coated tissue culture dishes in growth media. After 24 h, the media was changed to differentiation media consisting of Hams F-10/2% horse serum and incubated for an additional 60 h. Timepoints were taken at 24 h in growth media and at 12, 24, 36, 48 and 60 h in differentiation media. For clonal analysis, myoblasts were plated at 300 cells/dish. Differentiation was induced 4 days later, and 100 colonies were counted per dish with each timepoint being counted in triplicate.

Western blot analysis

Proliferating or differentiating myoblasts were lysed in NP-40 lysis buffer (50 mM Tris–HCl pH 8.0, 150 mM NaCl, 1% NP-40) with 1× protease inhibitors (Roche cat. no. 1 873 580). Proteins were separated using 5, 8, 10 or 12% SDS–PAGE gels in SDS–PAGE buffer (25 mM Tris–HCl pH 8.3, 192 mM glycine, 0.1% SDS) and transferred to nitrocellulose (0.45 μM, BioRad cat. no. 162-0145) in transfer buffer (25 mM Tris, 192 mM glycine, 15% methanol, pH 8.3). For emerin protein analyses, tissues were lysed with 7 M urea, 2 M thiourea, 2% Triton-X, 100 mM DTT, 1× and complete protease inhibitor cocktail (Roche) and separated on 12.5% denaturing acrylamide gels. Proteins were transferred to PVDF membranes. Proteins were detected using SuperSignal West Pico Chemiluminescent Substrate (Pierce). For Rb1 phosphorylation studies, muscles were homogenized in lysis buffer (50 mM HEPES–NaOH pH 7.5, 1% NP-40, 150 mM $NaCl_2$, 1 mM EDTA, 2.5 mM EGTA, 10% glycerol, 50 mM μ-glycerophosphate, 200 mM PMSF, 10 μg/ml aprotinin, 10 μg/ml leupeptin, 10 nM okadaic acid, 100 μM Na_3VO_4 and 1 μM microcyctin LR), spun at 10 000*g* for 10 min and protein content was determined using the DC protein assay. Supernatants were aliquoted (40 μg of total protein) and incubated with 2× Laemmli sample buffer, boiled and subjected to SDS–PAGE for subsequent western blotting. Rb was detected using an anti-Rb antibody (Pharmingen, San Diego, CA, USA) at 1:500, followed by incubation with an anti-mouse secondary antibody conjugated to horseradish peroxidase (1:10 000). Protein immunoblots were visualized by enhanced chemiluminescence. The sizes of the immunodetected proteins were verified using standard molecular weight markers.

Muscle degeneration/regeneration assay

Ctx was injected into both gastrocnemii of 12–16 week Emd−/Y-deficient mice, using a 10-needle manifold covering $1\ cm^2$ as previously described (32,33). Age- and sex-matched normal controls, as well as *Lmna*−/− mice (with appropriate controls) were assayed in parallel. Mice were euthanized at either 3 or 4 days during regeneration, tissues flash frozen and used for expression profiling, RT–PCR and protein studies.

Gastrocnemius muscles of indicated mouse strains at specific timepoints following CTX injection were harvested and used for histology, microarray analyses, immunoblotting and immunohistochemistry. Both gastrocnemii of three animals per strain and per timepoint were studied (six muscles). Emerin animals were 8 weeks old, the same age as those used for the previous multiple timepoint regeneration analysis to which they were to be compared. Because *Lmna*−/− animals have a severe phenotype that begins to be apparent around 5 weeks, we used 3–5-week-old animals and littermate controls of the same age.

For microarray studies, all six muscles per timepoint per strain were histologically examined by H+E and then three muscles selected for each strain and timepoint, which showed the most consistent degeneration/regeneration. Muscles were then ground in a mortar and pestle (cooled in liquid nitrogen) and RNA was prepared using the Qiagen RNAeasy fibrous tissue minikit. cRNA for chip analysis was prepared according to the manufacturer's directions, and chip analysis was done as previously described (64), following quality control and signal/noise optimization metrics that were previously described (65,66).

Immunohistochemistry analysis

Serial 6 μm-thick frozen muscle sections were cut with an IEC Minotome cryostat, mounted to Superfrost Plus Slides (Fisher Scientific) and fixed in cold anhydrous acetone. Sections were then blocked for 30 min in 10% horse serum and 1× PBS and incubated with a 1:50 dilution of mouse monoclonal antibody against embMHC (Iowa University) for 3 h at room temperature. Washes were done with 10% horse serum and 1× PBS and sections were then incubated with Cy3-conjugated goat anti-mouse antibody (Jackson Immunoresearch Inc.) at a 1:500 dilution for 1 h.

Real-time-RT–PCR

Two hundred nanograms of total RNA was reverse transcribed into single-stranded cDNA and aliquots (10 ng) processed for real-time-PCR. Fluorophore-labeled LUX primers were designed with LUX Designer software (www.invitrogen.com/lux) and purchased from Invitrogen. Affymetrix probe sets sequences were used as templates for primer design. Amplification and detection were done with ABI PRISM 7700 Sequence detector system (Applied Biosystems).

ACKNOWLEDGEMENTS

The authors wish to thank Dr Matt Guille for his generous supply of the Nap1L1 antibody and Roland Foisner for the anti-Lap2 antibodies. This research was supported by the Intramural Research Program of the National Cancer Institute and supported by grants from the NIH (NINDS 3RO1 NS29525-13; NICHD R21 HD044891-01), the Muscular Dystrophy Association and donations from the Crystal Ball

(Richmond, V.A.; Muscular Dystrophy Association) and Federation to Eradicate Duchenne (Washington DC).

Conflict of Interest statement. None declared.

REFERENCES

1. Dalkilic, I. and Kunkel, L.M. (2003) Muscular dystrophies: genes to pathogenesis. *Curr. Opin. Genet. Dev.*, **13**, 231–238.
2. Muntoni, F. and Voit, T. (2004) The congenital muscular dystrophies in 2004: a century of exciting progress. *Neuromuscul. Disord.*, **14**, 635–649.
3. Emery, A.E. and Dreifuss, F.E. (1966) Unusual type of benign x-linked muscular dystrophy. *J. Neurol. Neurosurg. Psychiatr.*, **29**, 338–342.
4. Bione, S., Maestrini, E., Rivella, S., Mancini, M., Regis, S., Romeo, G. and Toniolo, D. (1994) Identification of a novel X-linked gene responsible for Emery–Dreifuss muscular dystrophy. *Nat. Genet.*, **8**, 323–327.
5. Bonne, G., Di Barletta, M.R., Varnous, S., Becane, H.M., Hammouda, E.H., Merlini, L., Muntoni, F., Greenberg, C.R., Gary, F., Urtizberea, J.A. *et al.* (1999) Mutations in the gene encoding lamin A/C cause autosomal dominant Emery–Dreifuss muscular dystrophy. *Nat. Genet.*, **21**, 285–288.
6. Bonne, G., Mercuri, E., Muchir, A., Urtizberea, A., Becane, H.M., Recan, D., Merlini, L., Wehnert, M., Boor, R., Reuner, U. *et al.* (2000) Clinical and molecular genetic spectrum of autosomal dominant Emery–Dreifuss muscular dystrophy due to mutations of the lamin A/C gene. *Ann. Neurol.*, **48**, 170–180.
7. Burke, B. and Stewart, C.L. (2002) Life at the edge: the nuclear envelope and human disease. *Nat. Rev. Mol. Cell Biol.*, **3**, 575–585.
8. Hutchison, C.J. and Worman, H.J. (2004) A-type lamins: guardians of the soma? *Nat. Cell Biol.*, **6**, 1062–1067.
9. Mounkes, L. and Stewart, C.L. (2004) Structural organization and functions of the nucleus in development, aging, and disease. *Curr. Top. Dev. Biol.*, **61**, 191–228.
10. Lattanzi, G., Ognibene, A., Sabatelli, P., Capanni, C., Toniolo, D., Columbaro, M., Santi, S., Riccio, M., Merlini, L., Maraldi, N.M. *et al.* (2000) Emerin expression at the early stages of myogenic differentiation. *Differentiation*, **66**, 208–217.
11. Bengtsson, L. and Wilson, K.L. (2004) Multiple and surprising new functions for emerin, a nuclear membrane protein. *Curr. Opin. Cell Biol.*, **16**, 73–79.
12. Laguri, C., Gilquin, B., Wolff, N., Romi-Lebrun, R., Courchay, K., Callebaut, I., Worman, H.J. and Zinn-Justin, S. (2001) Structural characterization of the LEM motif common to three human inner nuclear membrane proteins. *Structure (Camb)*, **9**, 503–511.
13. Lee, K.K. and Wilson, K.L. (2004) All in the family: evidence for four new LEM-domain proteins Lem2 (NET-25), Lem3, Lem4 and Lem5 in the human genome. *Symp. Soc. Exp. Biol.*, **56**, 329–339.
14. Hutchison, C.J. (2002) Lamins: building blocks or regulators of gene expression? *Nat. Rev. Mol. Cell Biol.*, **3**, 848–858.
15. Gruenbaum, Y., Margalit, A., Goldman, R.D., Shumaker, D.K. and Wilson, K.L. (2005) The nuclear lamina comes of age. *Nat. Rev. Mol. Cell Biol.*, **6**, 21–31.
16. Ostlund, C., Bonne, G., Schwartz, K. and Worman, H.J. (2001) Properties of lamin A mutants found in Emery–Dreifuss muscular dystrophy, cardiomyopathy and Dunnigan-type partial lipodystrophy. *J. Cell Sci.*, **114**, 4435–4445.
17. Raharjo, W.H., Enarson, P., Sullivan, T., Stewart, C.L. and Burke, B. (2001) Nuclear envelope defects associated with LMNA mutations cause dilated cardiomyopathy and Emery–Dreifuss muscular dystrophy. *J. Cell Sci.*, **114**, 4447–4457.
18. Sullivan, T., Escalante-Alcalde, D., Bhatt, H., Anver, M., Bhat, N., Nagashima, K., Stewart, C.L. and Burke, B. (1999) Loss of A-type lamin expression compromises nuclear envelope integrity leading to muscular dystrophy. *J. Cell Biol.*, **147**, 913–920.
19. Grattan, M.J., Kondo, C., Thurston, J., Alakija, P., Burke, B.J., Stewart, C., Syme, D. and Giles, W.R. (2005) Skeletal and cardiac muscle defects in a murine model of Emery–Dreifuss muscular dystrophy. *Novartis Found. Symp.*, **264**, 118–133.
20. Nikolova, V., Leimena, C., McMahon, A.C., Tan, J.C., Chandar, S., Jogia, D., Kesteven, S.H., Michalicek, J., Otway, R., Verheyen, F. *et al.* (2004) Defects in nuclear structure and function promote dilated cardiomyopathy in lamin A/C-deficient mice. *J. Clin. Invest.*, **113**, 357–369.
21. Johnson, B.R., Nitta, R.T., Frock, R.L., Mounkes, L., Barbie, D.A., Stewart, C.L., Harlow, E. and Kennedy, B.K. (2004) A-type lamins regulate retinoblastoma protein function by promoting subnuclear localization and preventing proteasomal degradation. *Proc. Natl Acad. Sci. USA*, **101**, 9677–9682.
22. Markiewicz, E., Dechat, T., Foisner, R., Quinlan, R.A. and Hutchison, C.J. (2002) Lamin A/C binding protein LAP2alpha is required for nuclear anchorage of retinoblastoma protein. *Mol. Biol. Cell*, **13**, 4401–4413.
23. Bakay, M., Melcon, G., Wang, Z., Schiltz, L., Xuan, J., Zhao, P., Sartorelli, V., Seo, J., Pegoraro, E., Angelini, C. *et al.* (2006) Nuclear envelope dystrophies show a transcriptional fingerprint suggesting disruption of Rb–MyoD pathways in muscle regeneration. *Brain*, in press.
24. Jacks, T., Fazeli, A., Schmitt, E.M., Bronson, R.T., Goodell, M.A. and Weinberg, R.A. (1992) Effects of an Rb mutation in the mouse. *Nature*, **359**, 295–300.
25. Wu, L., de Bruin, A., Saavedra, H.I., Starovic, M., Trimboli, A., Yang, Y., Opavska, J., Wilson, P., Thompson, J.C., Ostrowski, M.C. *et al.* (2003) Extra-embryonic function of Rb is essential for embryonic development and viability. *Nature*, **421**, 942–947.
26. Huh, M.S., Parker, M.H., Scime, A., Parks, R. and Rudnicki, M.A. (2004) Rb is required for progression through myogenic differentiation but not maintenance of terminal differentiation. *J. Cell Biol.*, **166**, 865–876.
27. Zacksenhaus, E., Jiang, Z., Chung, D., Marth, J.D., Phillips, R.A. and Gallie, B.L. (1996) pRb controls proliferation, differentiation, and death of skeletal muscle cells and other lineages during embryogenesis. *Genes Dev.*, **10**, 3051–3064.
28. Puri, P.L., Iezzi, S., Stiegler, P., Chen, T.T., Schiltz, R.L., Muscat, G.E., Giordano, A., Kedes, L., Wang, J.Y. and Sartorelli, V. (2001) Class I histone deacetylases sequentially interact with MyoD and pRb during skeletal myogenesis. *Mol. Cell*, **8**, 885–897.
29. Iezzi, S., Cossu, G., Nervi, C., Sartorelli, V. and Puri, P.L. (2002) Stage-specific modulation of skeletal myogenesis by inhibitors of nuclear deacetylases. *Proc. Natl Acad. Sci. USA*, **99**, 7757–7762.
30. Puri, P.L., Sartorelli, V., Yang, X.J., Hamamori, Y., Ogryzko, V.V., Howard, B.H., Kedes, L., Wang, J.Y., Graessmann, A., Nakatani, Y. *et al.* (1997) Differential roles of p300 and PCAF acetyltransferases in muscle differentiation. *Mol. Cell*, **1**, 35–45.
31. Sartorelli, V., Puri, P.L., Hamamori, Y., Ogryzko, V., Chung, G., Nakatani, Y., Wang, J.Y. and Kedes, L. (1999) Acetylation of MyoD directed by PCAF is necessary for the execution of the muscle program. *Mol. Cell*, **4**, 725–734.
32. Zhao, P., Iezzi, S., Carver, E., Dressman, D., Gridley, T., Sartorelli, V. and Hoffman, E.P. (2002) Slug is a novel downstream target of MyoD. Temporal profiling in muscle regeneration. *J. Biol. Chem.*, **277**, 30091–30101.
33. Zhao, P., Seo, J., Wang, Z., Wang, Y., Shneiderman, B. and Hoffman, E.P. (2003) *In vivo* filtering of *in vitro* expression data reveals MyoD targets. *C. R. Biol.*, **326**, 1049–1065.
34. Steer, W.M., Abu-Daya, A., Brickwood, S.J., Mumford, K.L., Jordanaires, N., Mitchell, J., Robinson, C., Thorne, A.W. and Guille, M.J. (2003) Xenopus nucleosome assembly protein becomes tissue-restricted during development and can alter the expression of specific genes. *Mech. Dev.*, **120**, 1045–1057.
35. Muchir, A., van Engelen, B.G., Lammens, M., Mislow, J.M., McNally, E., Schwartz, K. and Bonne, G. (2003) Nuclear envelope alterations in fibroblasts from LGMD1B patients carrying nonsense Y259X heterozygous or homozygous mutation in lamin A/C gene. *Exp. Cell Res.*, **291**, 352–362.
36. Black, E.P., Huang, E., Dressman, H., Rempel, R., Laakso, N., Asa, S.L., Ishida, S., West, M. and Nevins, J.R. (2003) Distinct gene expression phenotypes of cells lacking Rb and Rb family members. *Cancer Res.*, **63**, 3716–3723.
37. Markey, M.P., Angus, S.P., Strobeck, M.W., Williams, S.L., Gunawardena, R.W., Aronow, B.J. and Knudsen, E.S. (2002) Unbiased analysis of RB-mediated transcriptional repression identifies novel targets and distinctions from E2F action. *Cancer Res.*, **62**, 6587–6597.
38. Young, A.P., Nagarajan, R. and Longmore, G.D. (2003) Mechanisms of transcriptional regulation by Rb-E2F segregate by biological pathway. *Oncogene*, **22**, 7209–7217.

39. Ait-Si-Ali, S., Guasconi, V., Fritsch, L., Yahi, H., Sekhri, R., Naguibneva, I., Robin, P., Cabon, F., Polesskaya, A. and Harel-Bellan, A. (2004) A Suv39 h-dependent mechanism for silencing S-phase genes in differentiating but not in cycling cells. *EMBO J.*, **23**, 605–615.
40. Luo, R.X., Postigo, A.A. and Dean, D.C. (1998) Rb interacts with histone deacetylase to repress transcription. *Cell*, **92**, 463–473.
41. Narita, M., Nunez, S., Heard, E., Lin, A.W., Hearn, S.A., Spector, D.L., Hannon, G.J. and Lowe, S.W. (2003) Rb-mediated heterochromatin formation and silencing of E2F target genes during cellular senescence. *Cell*, **113**, 703–716.
42. Nielsen, S.J., Schneider, R., Bauer, U.M., Bannister, A.J., Morrison, A., O'Carroll, D., Firestein, R., Cleary, M., Jenuwein, T., Herrera, R.E. *et al.* (2001) Rb targets histone H3 methylation and HP1 to promoters. *Nature*, **412**, 561–565.
43. Ringrose, L. and Paro, R. (2001) Remembering silence. *Bioessays*, **23**, 566–570.
44. Dunaief, J.L., Strober, B.E., Guha, S., Khavari, P.A., Alin, K., Luban, J., Begemann, M., Crabtree, G.R. and Goff, S.P. (1994) The retinoblastoma protein and BRG1 form a complex and cooperate to induce cell cycle arrest. *Cell*, **79**, 119–130.
45. Robertson, K.D., Ait-Si-Ali, S., Yokochi, T., Wade, P.A., Jones, P.L. and Wolffe, A.P. (2000) DNMT1 forms a complex with Rb, E2F1 and HDAC1 and represses transcription from E2F-responsive promoters. *Nat. Genet.*, **25**, 338–342.
46. Clegg, C.H., Linkhart, T.A., Olwin, B.B. and Hauschka, S.D. (1987) Growth factor control of skeletal muscle differentiation: commitment to terminal differentiation occurs in G1 phase and is repressed by fibroblast growth factor. *J. Cell Biol.*, **105**, 949–956.
47. Maidment, S.L. and Ellis, J.A. (2002) Muscular dystrophies, dilated cardiomyopathy, lipodystrophy and neuropathy: the nuclear connection. *Expert. Rev. Mol. Med.*, **4**, 1–21.
48. Magenta, A., Cenciarelli, C., De Santa, F., Fuschi, P., Martelli, F., Caruso, M. and Felsani, A. (2003) MyoD stimulates RB promoter activity via the CREB/p300 nuclear transduction pathway. *Mol. Cell Biol.*, **23**, 2893–2906.
49. Mal, A. and Harter, M.L. (2003) MyoD is functionally linked to the silencing of a muscle-specific regulatory gene prior to skeletal myogenesis. *Proc. Natl Acad. Sci. USA*, **100**, 1735–1739.
50. Mal, A., Sturniolo, M., Schiltz, R.L., Ghosh, M.K. and Harter, M.L. (2001) A role for histone deacetylase HDAC1 in modulating the transcriptional activity of MyoD: inhibition of the myogenic program. *EMBO J.*, **20**, 1739–1753.
51. Markiewicz, E., Ledran, M. and Hutchison, C.J. (2005) Remodelling of the nuclear lamina and nucleoskeleton is required for skeletal muscle differentiation *in vitro*. *J. Cell Sci.*, **118**, 409–420.
52. Somech, R., Shaklai, S., Geller, O., Amariglio, N., Simon, A.J., Rechavi, G. and Gal-Yam, E.N. (2005) The nuclear-envelope protein and transcriptional repressor LAP2{beta} interacts with HDAC3 at the nuclear periphery, and induces histone H4 deacetylation. *J. Cell Sci.*, **118**, 4017–4025.
53. Favreau, C., Higuet, D., Courvalin, J.C. and Buendia, B. (2004) Expression of a mutant lamin A that causes Emery–Dreifuss muscular dystrophy inhibits *in vitro* differentiation of C2C12 myoblasts. *Mol. Cell Biol.*, **24**, 1481–1492.
54. Lammerding, J., Schulze, P.C., Takahashi, T., Kozlov, S., Sullivan, T., Kamm, R.D., Stewart, C.L. and Lee, R.T. (2004) Lamin A/C deficiency causes defective nuclear mechanics and mechanotransduction. *J. Clin. Invest.*, **113**, 370–378.
55. Lammerding, J., Hsiao, J., Schulze, P.C., Kozlov, S., Stewart, C.L. and Lee, R.T. (2005) Abnormal nuclear shape and impaired mechanotransduction in emerin-deficient cells. *J. Cell Biol.*, **170**, 781–791.
56. Harbour, J.W., Luo, R.X., Dei Santi, A., Postigo, A.A. and Dean, D.C. (1999) Cdk phosphorylation triggers sequential intramolecular interactions that progressively block Rb functions as cells move through G1. *Cell*, **98**, 859–869.
57. Flemington, E.K., Speck, S.H. and Kaelin, W.G., Jr. (1993) E2F-1-mediated transactivation is inhibited by complex formation with the retinoblastoma susceptibility gene product. *Proc. Natl Acad. Sci. USA*, **90**, 6914–6918.
58. Mal, A., Chattopadhyay, D., Ghosh, M.K., Poon, R.Y., Hunter, T. and Harter, M.L. (2000) p21 and retinoblastoma protein control the absence of DNA replication in terminally differentiated muscle cells. *J. Cell Biol.*, **149**, 281–292.
59. Polioudaki, H., Kourmouli, N., Drosou, V., Bakou, A., Theodoropoulos, P.A., Singh, P.B., Giannakouros, T. and Georgatos, S.D. (2001) Histones H3/H4 form a tight complex with the inner nuclear membrane protein LBR and heterochromatin protein 1. *EMBO Rep.*, **2**, 920–925.
60. Young, A.P. and Longmore, G.D. (2004) Differences in stability of repressor complexes at promoters underlie distinct roles for Rb family members. *Oncogene*, **23**, 814–823.
61. Lipinski, M.M. and Jacks, T. (1999) The retinoblastoma gene family in differentiation and development. *Oncogene*, **18**, 7873–7882.
62. Stewart, C.L. (1993) Production of chimeras between embryonic stem cells and embryos. *Methods Enzymol.*, **225**, 823–855.
63. Lewandoski, M. and Martin, G.R. (1997) Cre-mediated chromosome loss in mice. *Nat. Genet.*, **17**, 223–225.
64. Zhao, P. and Hoffman, E.P. (2004) Embryonic myogenesis pathways in muscle regeneration. *Dev. Dyn.*, **229**, 380–392.
65. Seo, J., Bakay, M., Chen, Y.W., Hilmer, S., Shneiderman, B. and Hoffman, E.P. (2004) Interactively optimizing signal-to-noise ratios in expression profiling: project-specific algorithm selection and detection *P*-value weighting in Affymetrix microarrays. *Bioinformatics*, **20**, 2534–2544.
66. The Tumor Analysis Best Practices Working Group (2004) Expression profiling—Best practices for data generation and interpretations in clinical trials. *Nat. Rev. Genet.*, **5**, 229–237.